

DIAGNOSIS OF THE PERFORMANCE OF THE ECMWF FORECASTING SYSTEM IN THE STRATOSPHERE

E. Klinker (ECMWF)

1. INTRODUCTION

Soon after large scale analyses of stratospheric data became available it emerged that the winter time stratospheric circulation is mainly driven from the troposphere. Particularly the diagnosis of the energy cycle in the Lorenz formulation (Doplick, 1971 for the Northern Hemisphere and Hartmann, 1976 for the Southern Hemisphere) showed that boundary fluxes through the tropopause or through a low latitude lateral boundary were by far larger than internal energy sources which could account for the observed energy conversions in the stratosphere. The fact that large scale eddies in the stratosphere are mainly the result of vertically propagating planetary waves from the troposphere implies that forecast errors in the troposphere could propagate into the stratosphere during the winter season and may consequently affect the performance of the model in the stratosphere. The time sequence of root mean square errors for the winter 1992/93 indeed suggests a relation between stratospheric and tropospheric errors at day-10 of the forecast (Fig. 1). Large errors in the stratosphere are seen in phase with maximum errors in the troposphere. At a shorter forecast time of five days the correlation between stratospheric and tropospheric errors is, however, less pronounced.

For the diagnosis of the model performance in the stratosphere internal error sources are important as well, particularly during the summer season when the stratospheric circulation is dominated by radiative processes. Diabatic forcing errors and errors that arise from the reflection of planetary waves at the upper boundary may not only affect the performance of the model in the stratosphere. Downward propagation of stratospheric errors could contaminate tropospheric forecast parameters which are of more general use for weather forecasting than stratospheric forecast parameters itself. Therefore the question of forecast quality in the stratosphere has some implications for the model performance in the troposphere. Experience at ECMWF has shown that the medium range forecast quality in the troposphere depends to a certain extent on the vertical resolution of the model in the stratosphere and on the location of the upper boundary (Simmons, in these proceedings).

ECMWF FORECAST VERIFICATION 12Z

50hPa GEOPOTENTIAL

ROOT MEAN SQUARE ERROR FORECAST
 N.HEM LAT 20.000 TO 90.000 LON -180.000 TO 180.000

----- T+120 MA
 _____ T+240 MA

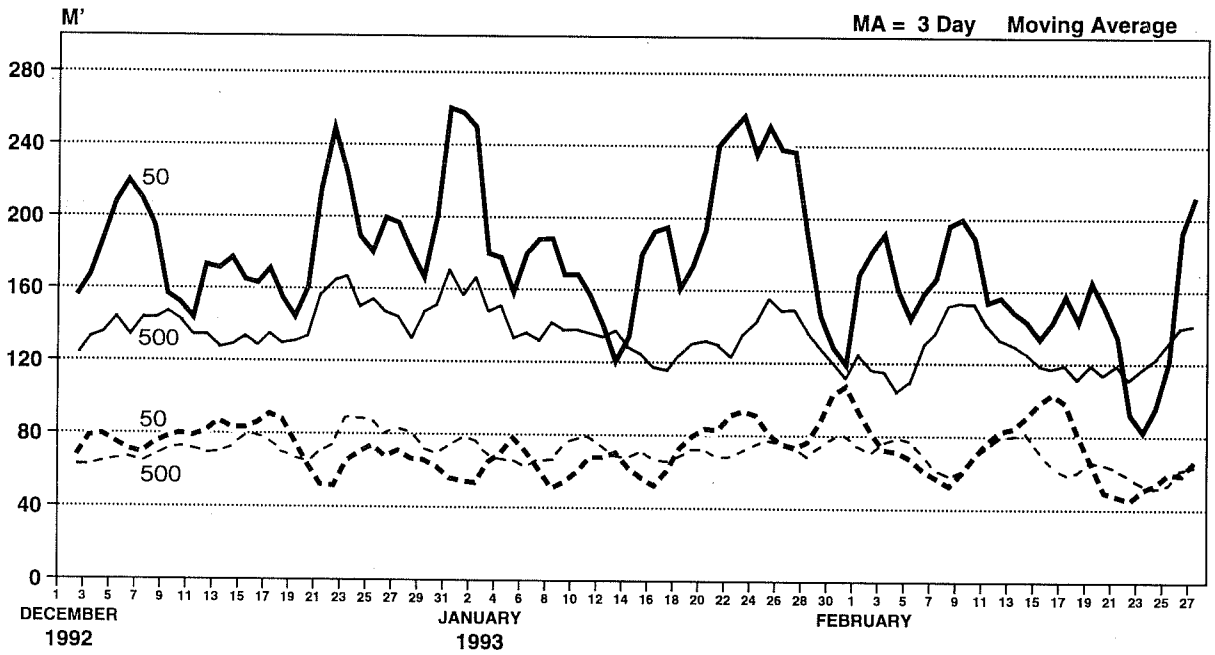


Fig. 1 Root mean square errors of day-5 and day-10 forecasts for 500 and 50 hPa in the winter 1992/93. units: m.

2. SYSTEMATIC ERRORS

2.1 Zonal mean errors

By averaging forecast errors zonally and over a period of a season it is hoped to obtain some information on possible model deficiencies. However, model errors on this time and space scale can still depend on seasonal variations. The sequence of zonal mean temperature errors for the four seasons, autumn 1992 to summer 1993 (Fig. 2), is a good example of exhibiting the influence of model changes and seasonal variations. Particularly large positive errors occur in the middle stratosphere in summer when the absorption of solar radiation causes a reversal of the circulation in this region. During winter the opposite error, excessive cooling, can be seen close to the model top layer.

Further down in the lower stratosphere the modification of the parametrization of radiation on 1 February 1993 had a noticeable impact. The revision of clear sky absorption coefficients and the inclusion of short wave optical properties for ice and mixed phase clouds led to a larger absorption of solar radiation in the atmosphere. The excessive upper tropospheric cooling as seen for (NH) autumn 1992 and winter 1992/93 has been reduced in the following seasons. However, a detrimental impact was felt in the lower stratosphere where a small positive error around 0.5 K at day-5 of the forecast increased to around 1.2 degrees in spring and summer 1993.

Systematic errors of the zonal wind have reached a fairly low level compared to previous years. At day-5 of the forecast (Fig. 3), a small increase of wind speed in the polar night jet compared to the analysis can be seen in both winter hemispheres, the errors reach a maximum of 10%. The tropical wind errors depend to a large extent on the phase of the QBO which itself is probably not captured by the analysis completely. Largest errors occur in autumn 1992 and winter 1992/93 when the west wind phase was descending from the middle to the lower stratosphere.

2.2 Longitudinal structure of systematic errors

Large contributions to the stratospheric and tropospheric large scale heat and momentum fluxes arise from stationary planetary waves. Fig. 4a shows in a longitude-height cross section the vertical structure of the stationary waves for the Northern Hemisphere winter season. The predominant westward tilt of troughs and ridges with height indicates a large contribution to the horizontal heat flux. The largest tilts are found in an area from East Europe to the East Pacific. Going further east, one notices that the ridges and troughs lose progressively their tilt, so that in the Atlantic-West-

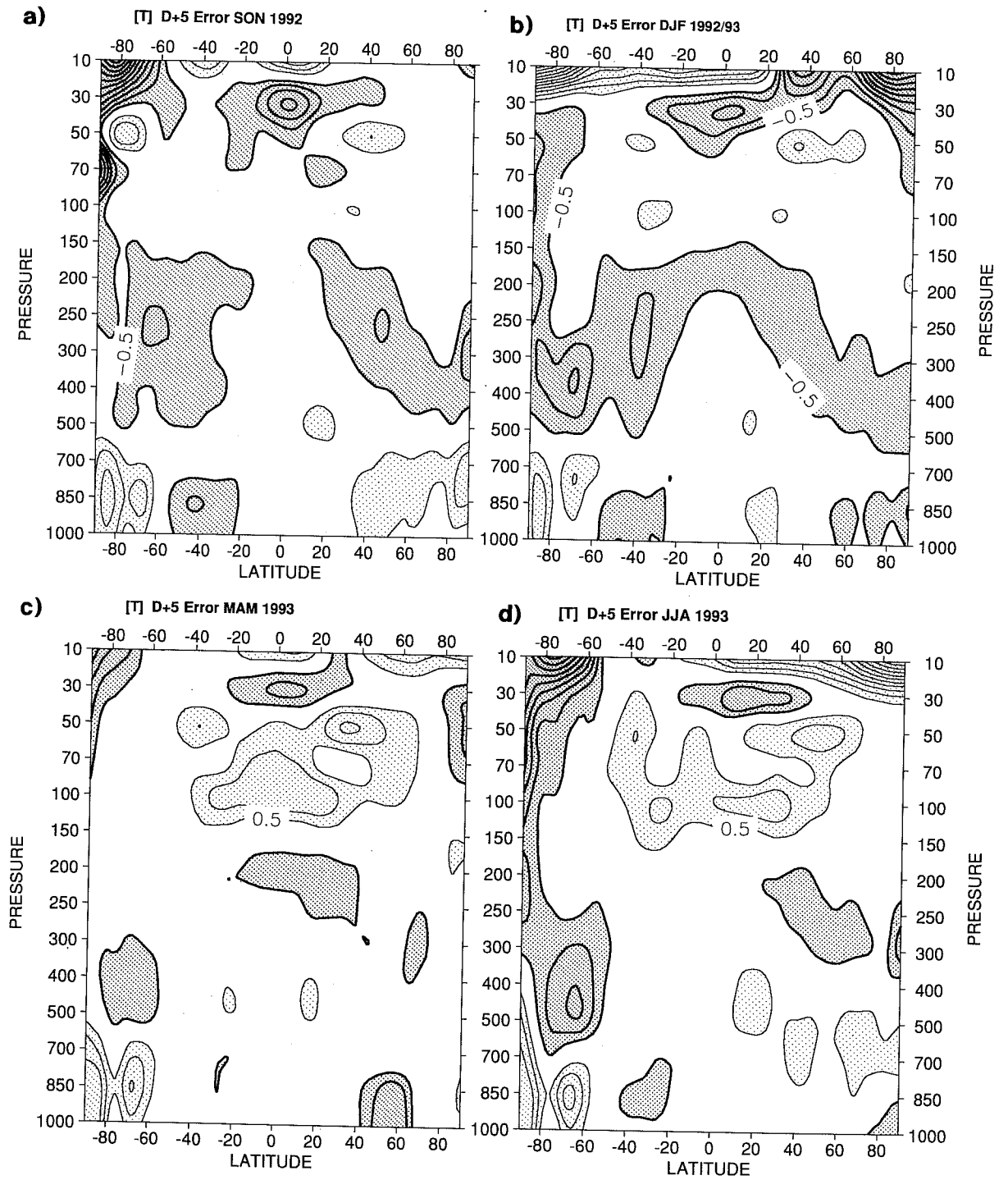


Fig. 2 Zonal mean temperature errors at day-5 for four seasons. (a) Autumn 1992, (b) winter 1992/93, (c) spring 1993, (d) summer 1993. Contour interval 0.5 K (light shading positive values).

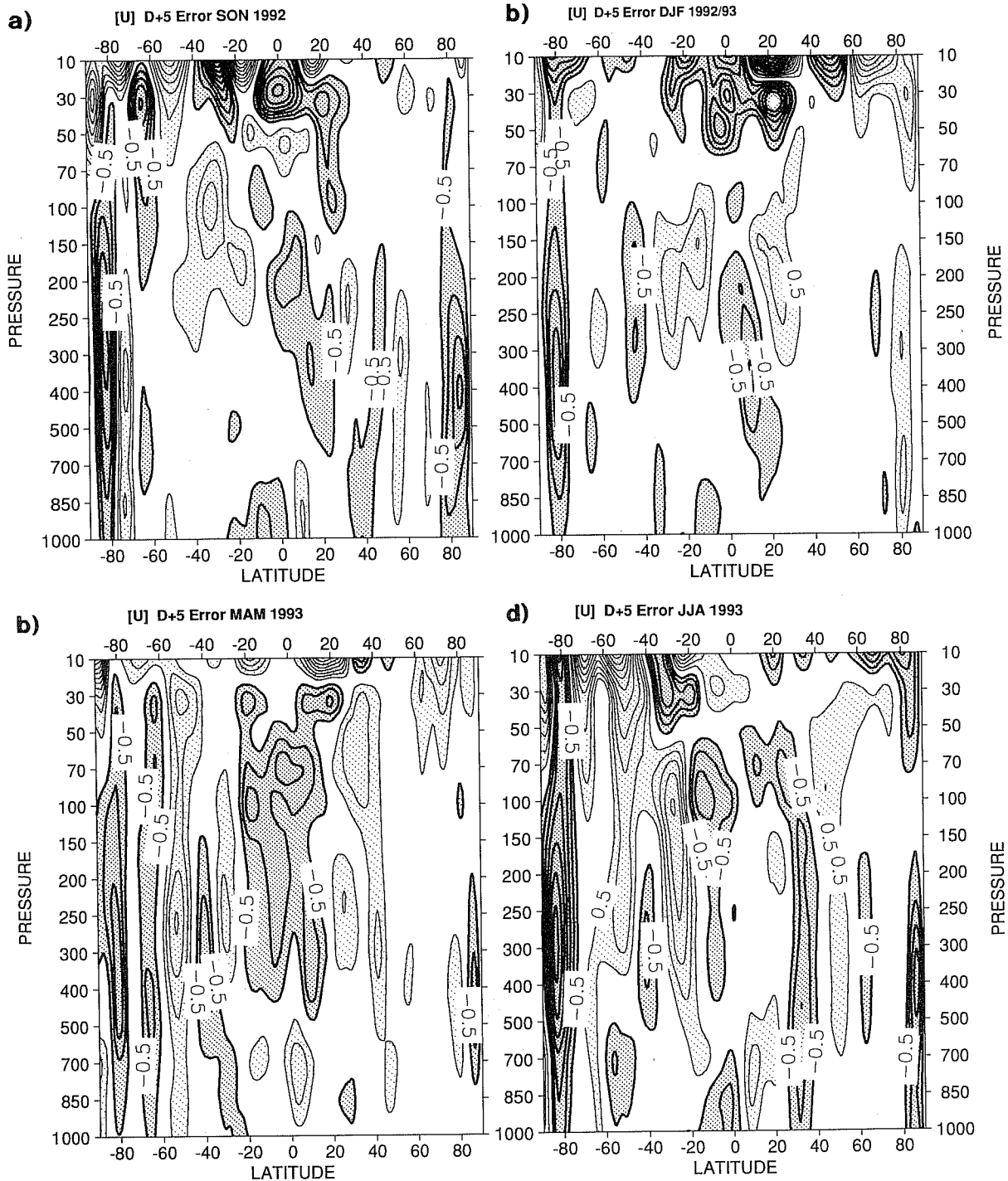


Fig. 3 Zonal mean wind errors at day-5 for four seasons. (a) Autumn 1992, (b) winter 1992/93, (c) spring 1993, (d) summer 1993. Contour interval 0.5 K (light shading positive values).

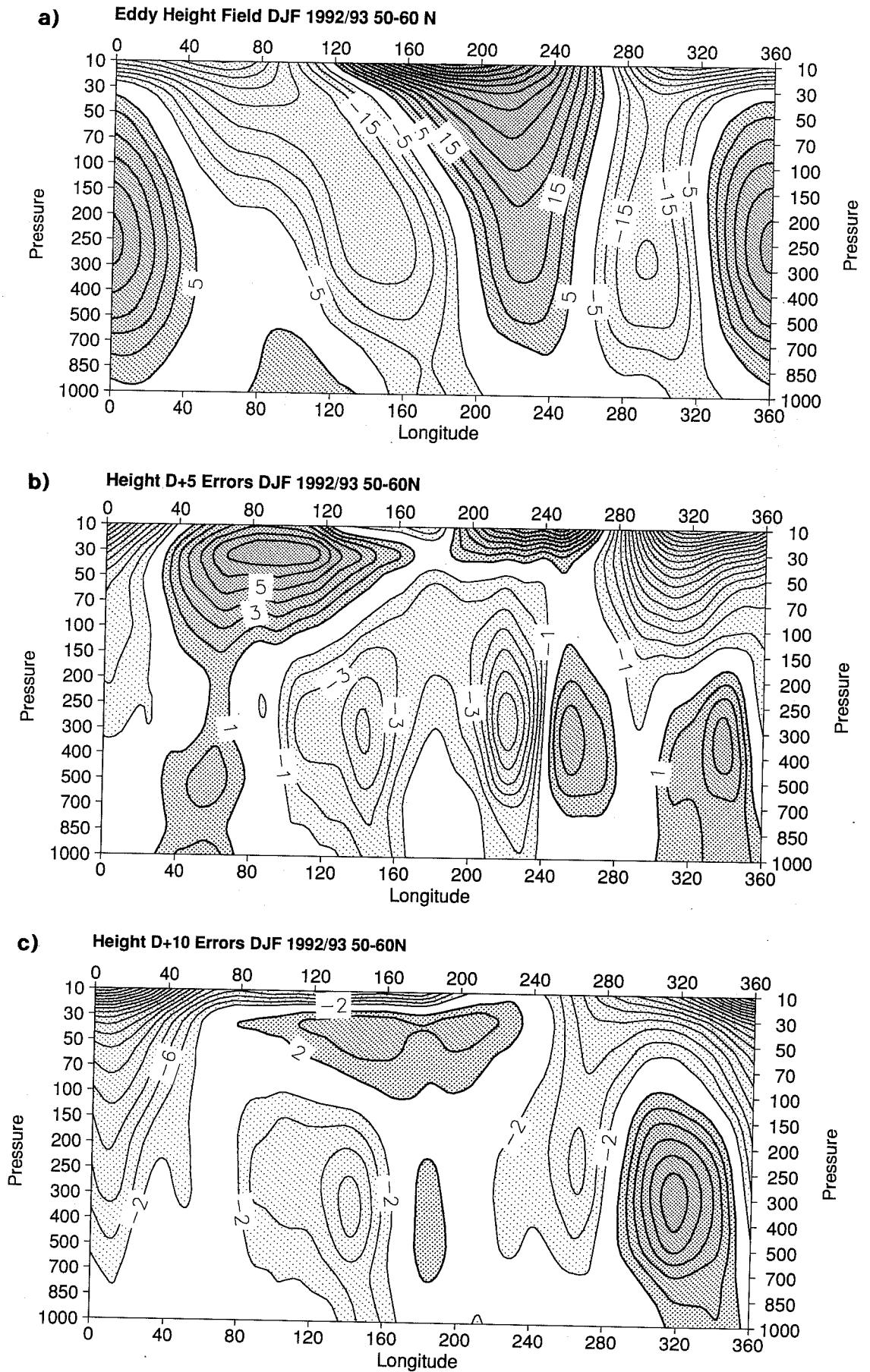


Fig. 4 Longitude-pressure cross sections of height for winter 1992/93 averaged over 50-60 degrees north. (a) Analysis values shown as departure from the zonal mean, (b) mean day-5 forecast errors, (c) mean day-10 forecast errors. Units: dam.

European area the phase lines of the stationary waves are almost vertically.

Errors of the stationary waves during the first five days of the forecast have a nearly quasi-linear behaviour in time, with amplitudes rising but with a fairly fixed phase structure in space. By day-5 of the forecast the largest errors in the troposphere are found in the vicinity of the East Pacific ridge that is weakened and slightly moved to the east (Fig. 4b). At the same time the model is deepening the West Pacific trough. Model biases in the stratosphere seem to have mainly the opposite sign compared to errors in the troposphere, with the largest errors in the Atlantic area indicating a deepening of the stratospheric trough.

During the next five days of forecast time leading up to day-10 nonlinear growth of errors contributes to larger longitudinal shifts of some of the major trough-ridge structures (Fig. 4c). In the troposphere the Pacific trough is further intensified whereas the Atlantic trough-ridge system has moved westward. In the stratosphere the height errors by day 10 are predominantly negative with largest values over the East-Atlantic European sector.

The European part of the longitude-pressure section is the only area where vertically coherent errors structures are found. The time evolution for the systematic height errors for the average over 0 to 30 degrees east and 50 to 60 degrees north (Fig. 5) shows that for this region large forecast errors that are initially only present in the stratosphere propagate down into the troposphere after day-6 of the forecast reaching maximum amplitudes by day-10. Boville and Baumhefner (1990) found a signal of vertically downward propagating errors in the East Atlantic area when they compared climate simulations using models with different vertical extent, one model including the mesosphere and the other model with a top below 10 hPa. As the Atlantic is an area where stratospheric warmings are often associated with the development of a secondary anticyclone apart from the Aleutian high, they speculate that this preferred region of vertical propagation of eddies into the stratosphere would also be a preferred region of downward propagation of reflected waves.

The structure of height errors in Fig. 4a and 4b implies a corresponding structure of temperature errors (Fig. 6a) via the hydrostatic relation. Whereas over the East-Atlantic area negative temperature errors extend over most of the upper troposphere and stratosphere, other areas show a large vertical gradient of temperature errors with positive errors in the lower stratosphere and negative errors close to the top level of the model. By day-10 of the forecast the structure of the temperature errors has changed only little, mainly the magnitude of errors has become larger (Fig. 6b). Deep upper stratospheric cooling has spread to Western Europe and negative temperature errors close to the top level of the model over the Asian continent and over the Pacific have penetrated further down into the lower stratosphere.

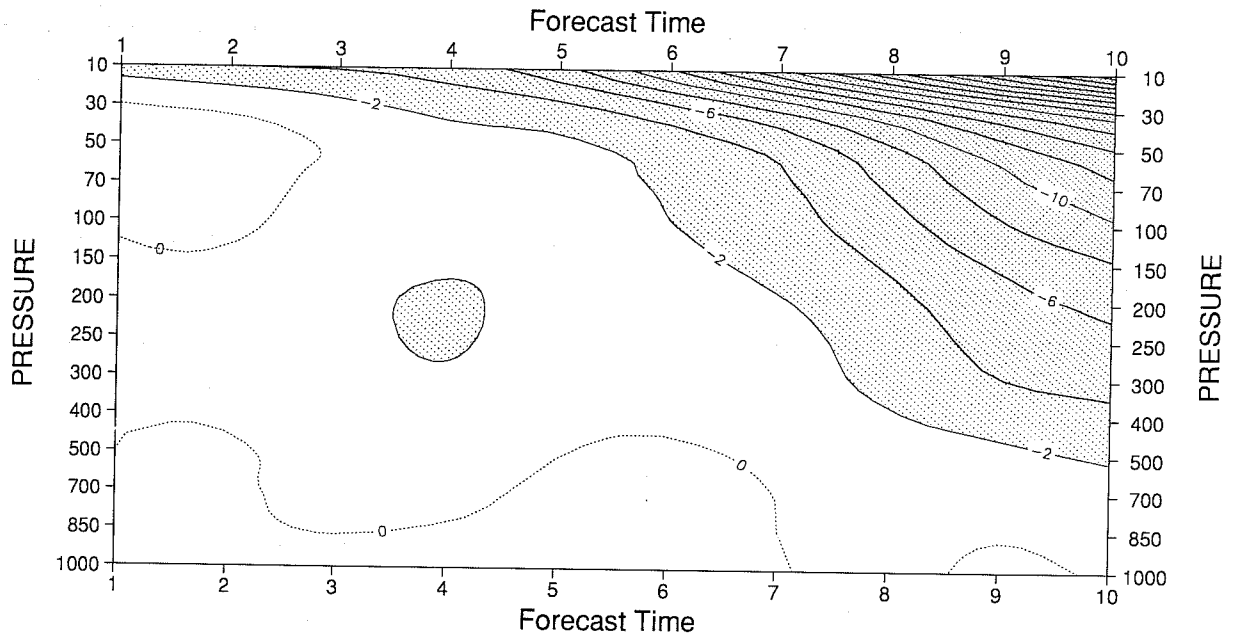


Fig. 5 Time-pressure cross section of mean height errors for an area over Europe (50-60N and 0-30E).
 Abscissa: forecast time in days. Units: dam.

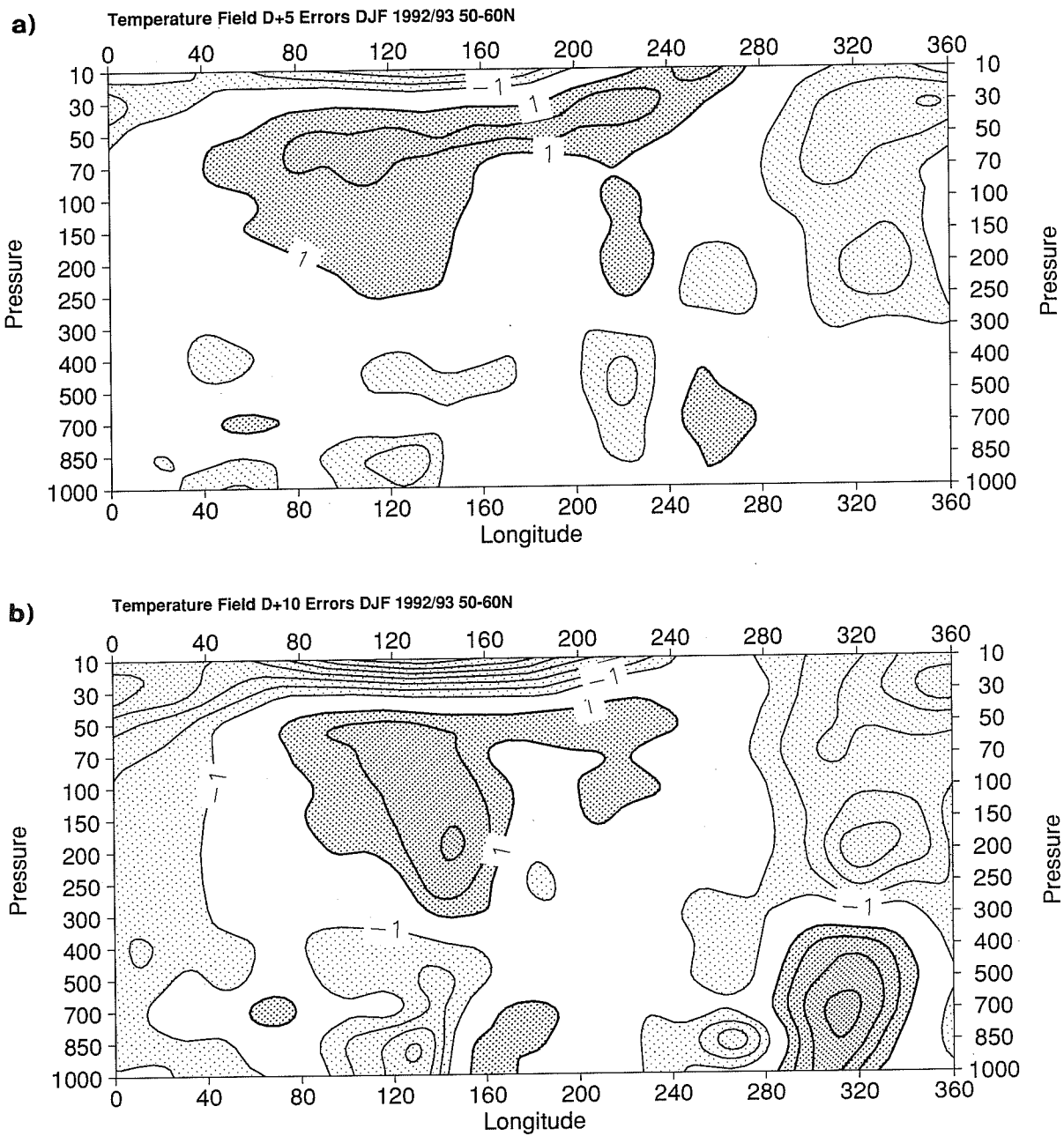


Fig. 6 Longitude-pressure cross sections of temperature errors for winter 1992/93 averaged over 50-60 degrees north. (a) mean day-5 forecast errors, (b) mean day-10 forecast errors. Units: K.

In the Southern Hemisphere winter the tropospheric flow pattern is much more zonally symmetric than the Northern Hemispheric flow (Fig. 7a). Therefore the stationary waves have a smaller amplitude in the troposphere and in the stratosphere compared to the Northern Hemisphere. As in the Northern Hemisphere, forecast errors in the Southern Hemisphere are growing fairly linear in time. Surprisingly, the positions of maximum errors in the day-5 forecast (Fig. 7b) and in the day-10 forecast (Fig. 7c) are fairly similar, particularly in the troposphere. At both forecast ranges (day-5 and day-10) systematic height errors in the Southern Hemisphere suggest a phase shift of the major troughs and ridges to the west. This phase shift extends rather uniform from the troposphere into the stratosphere, indicating a link between errors of the stratospheric and tropospheric eddies.

During the summer in the Northern Hemisphere the easterly flow in the stratosphere traps the stationary waves in the troposphere. In contrast to winter the amplitude of the eddy height field above 250 hPa (Fig. 8a) is decreasing with height. However, during the summer season the forecast performance in the stratosphere is characterized by comparatively large height errors (Fig. 8b) that appear to be fairly zonally symmetric. In the absence of large dynamical forcing from the troposphere the implied temperature errors suggest an imbalance between the radiative forcing and dynamical temperature tendencies.

3. RANDOM ERRORS

Though the diagnosis of systematic forecast errors is very useful for identifying specific model problems, time mean errors form only the smaller part of the total forecast errors. Therefore the standard deviations of forecasts from analyses are discussed and are used as a measure of non-systematic errors which will also be referred to as random errors.

The atmospheric variability is shown by the standard deviation of the analysis from the mean (Fig. 9a). At high latitudes (in a band from 50-60 degrees north) three major areas of eddy activity appear in the troposphere. The eastern Europe and Atlantic centres of variability which are located on the eastern and western side of the stationary West European ridge (see Fig. 6a) extend into the stratosphere. In contrast, the eddy activity located to the west of the North-American stationary ridge is more confined to the troposphere.

A spectral space filter has been used to separate the high and low wave-number regime of atmospheric waves. The separation has been done on the basis of the two dimensional spherical harmonic wave-number n . The low wave-number regime (defined by waves with total wave-number 1 to 6, Fig. 9b)

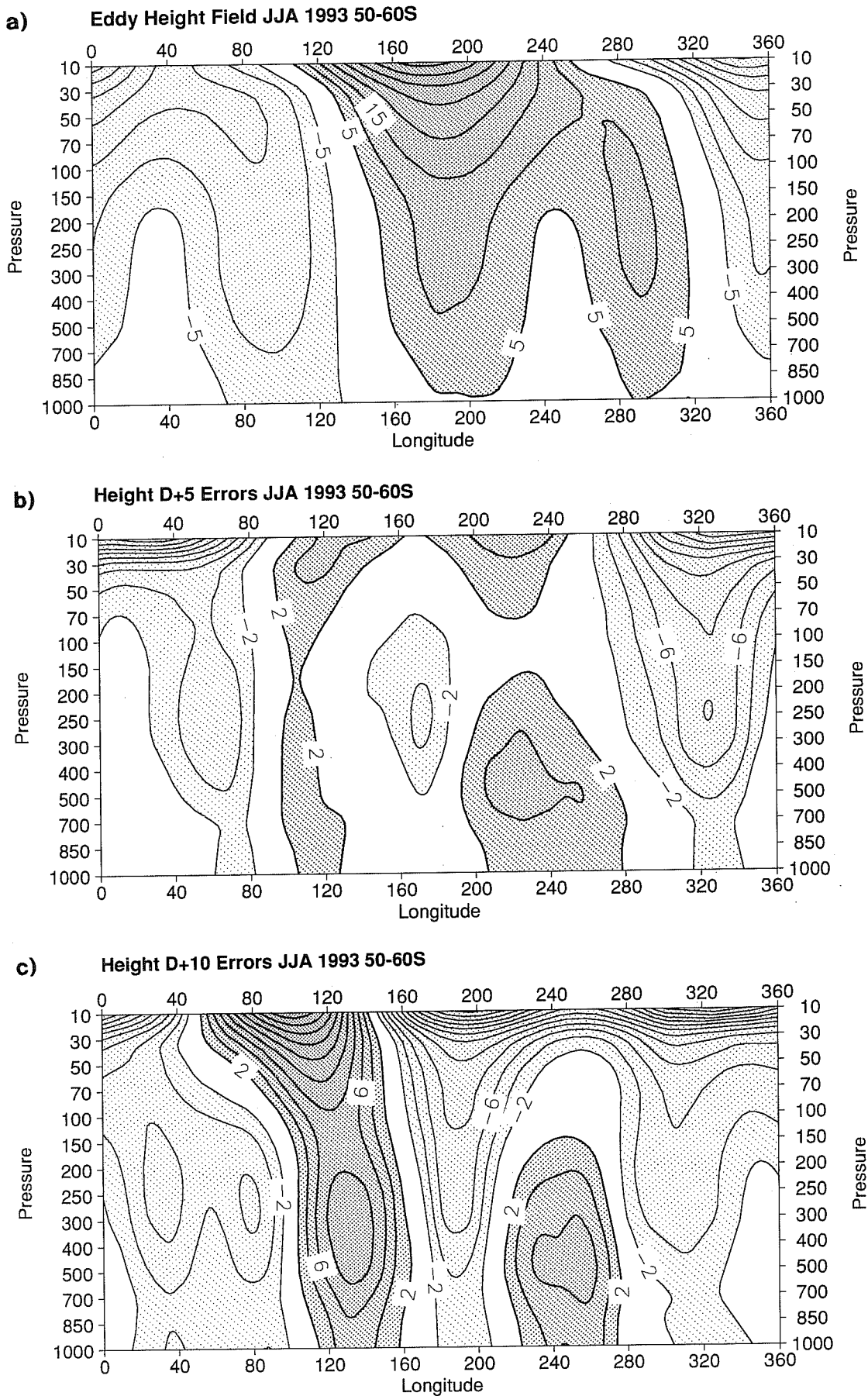


Fig. 7 Longitude-pressure cross sections of height for summer 1993 averaged over 50-60 degrees south. (a) Analysis as departure from zonal mean, (b) mean day-5 forecast errors, (c) mean day-10 forecast errors. Units: dam.

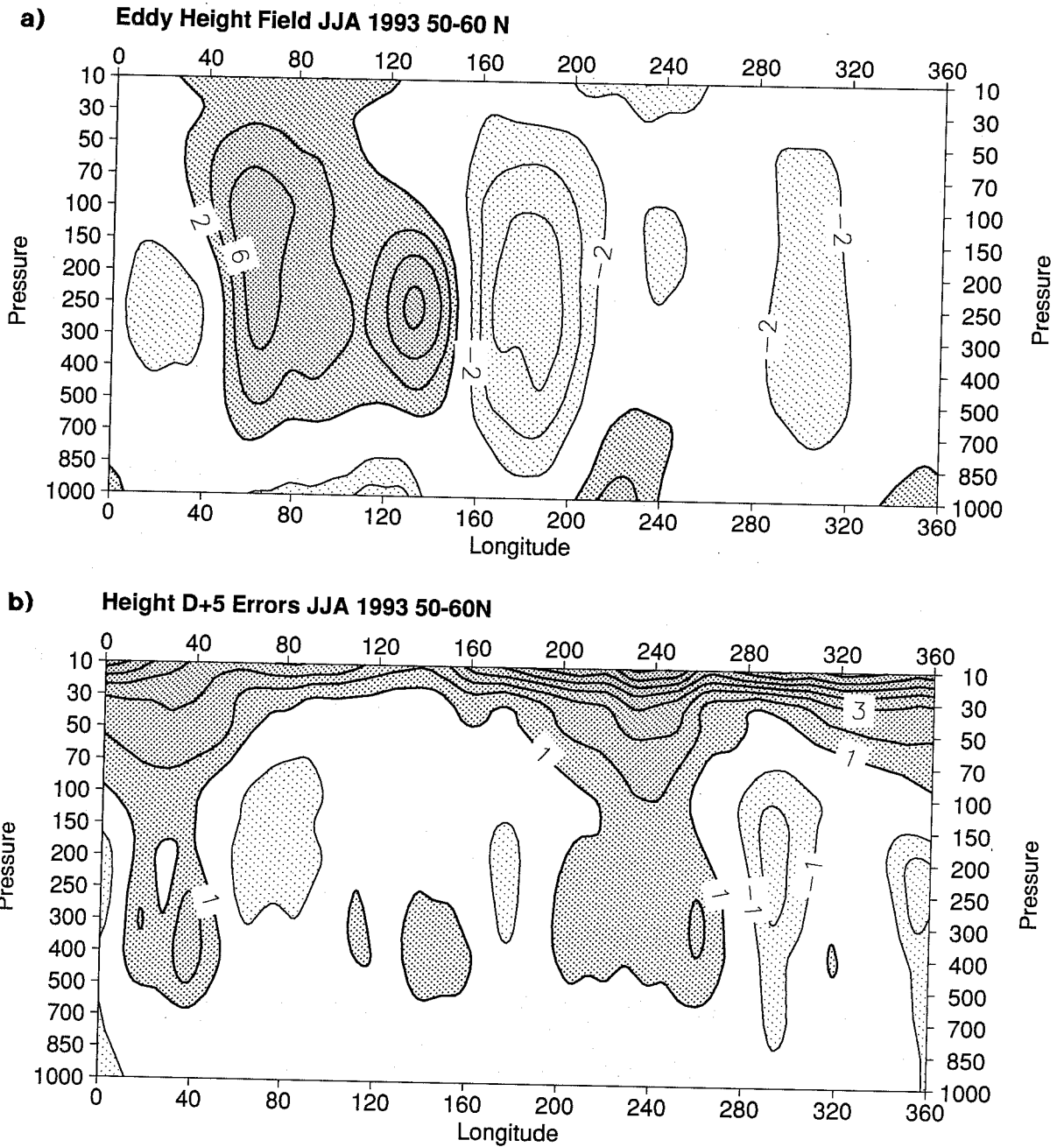


Fig. 8 Longitude-pressure cross sections of height for summer 1993 averaged over 50-60 degrees north. (a) Analysis as departure from zonal mean, (b) mean day-5 forecast errors. Units: dam.

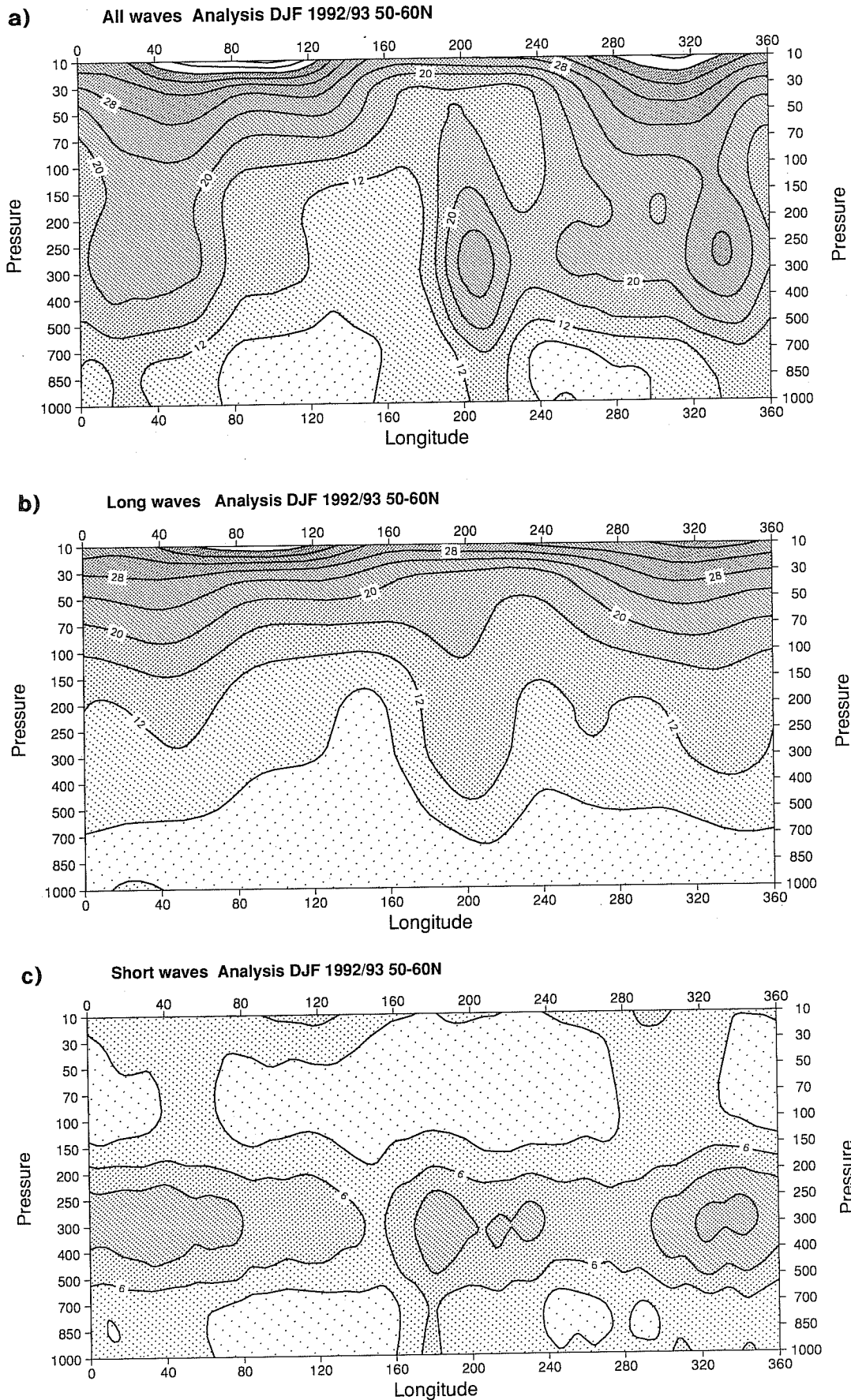


Fig. 9 Longitude-pressure cross section of height variability in terms of standard deviation from the seasonal mean for winter 1992/93. (a) all waves, (b) long waves (total wavenumber smaller than 7), (c) short waves (total wavenumber larger than 10). Units: dam.

receives its main contribution from quasi-stationary waves, whereas the high wave number regime (wave-number larger than 10, Fig. 9c) is dominated by the baroclinic waves.

Comparing the long and short wave-number domain it is obvious that the total standard deviation of height is dominated by long waves. Similar to the total standard deviation of height, the long wave variability shows three major maxima in the troposphere over eastern Europe, the East Pacific and the East Atlantic. The wave-number three structure of tropospheric variability is gradually changing with height to a two wave structure in the stratosphere. The reason for this is that the large variability associated with the East Pacific ridge is weakening with height. In synoptic terms it resembles the fact that the quasi-stationary Aleutian high in the stratosphere has a rather small variability in strength compared to the two troughs over eastern Europe and the Atlantic, which are more variable in position and intensity.

The fact that only long waves with zonal wave number one and two are able to propagate into the middle to upper stratosphere is well explained by theory (Charney and Drazin, 1961). Therefore it is not surprising to find the baroclinic waves, here defined as eddies with total wave number larger than 10, to be trapped in the troposphere. For the discussion of forecast errors in the stratosphere they seem to be less important than long waves.

The standard deviation of day-5 forecasts from analyses for all waves shows two areas of maximum random errors, the upper troposphere and the stratosphere close to the upper boundary of the model (Fig. 10a). The separation of forecast errors into contributions from long waves and short waves shows the dominance of errors from the long waves (Fig. 10b) in the stratosphere and of errors from the baroclinic waves (Fig. 10c) in the troposphere. It is, however, interesting to note that the same geographical areas give rise to maximum errors in the long and short wave-number regime.

The vertical structure of the forecast errors does not suggest an obvious link between tropospheric and stratospheric errors. However, the large vertical gradient of errors in the stratosphere with maximum errors occurring close to the top of the model can be seen as an indication of specific problems at the upper boundary of the model.

Evidence that vertical error propagation from the troposphere into the stratosphere is important for the medium forecast range can be seen from the time evolution of random errors. Fig. 11 shows the increase of long wave random errors normalized by the analyzed atmospheric variability (see Fig. 9b). Between day-1 and day-3 and day-3 and day-5 the largest normalized increase of long wave random errors takes place at low levels. Between day-5 and day-7 there is already a sign of vertical

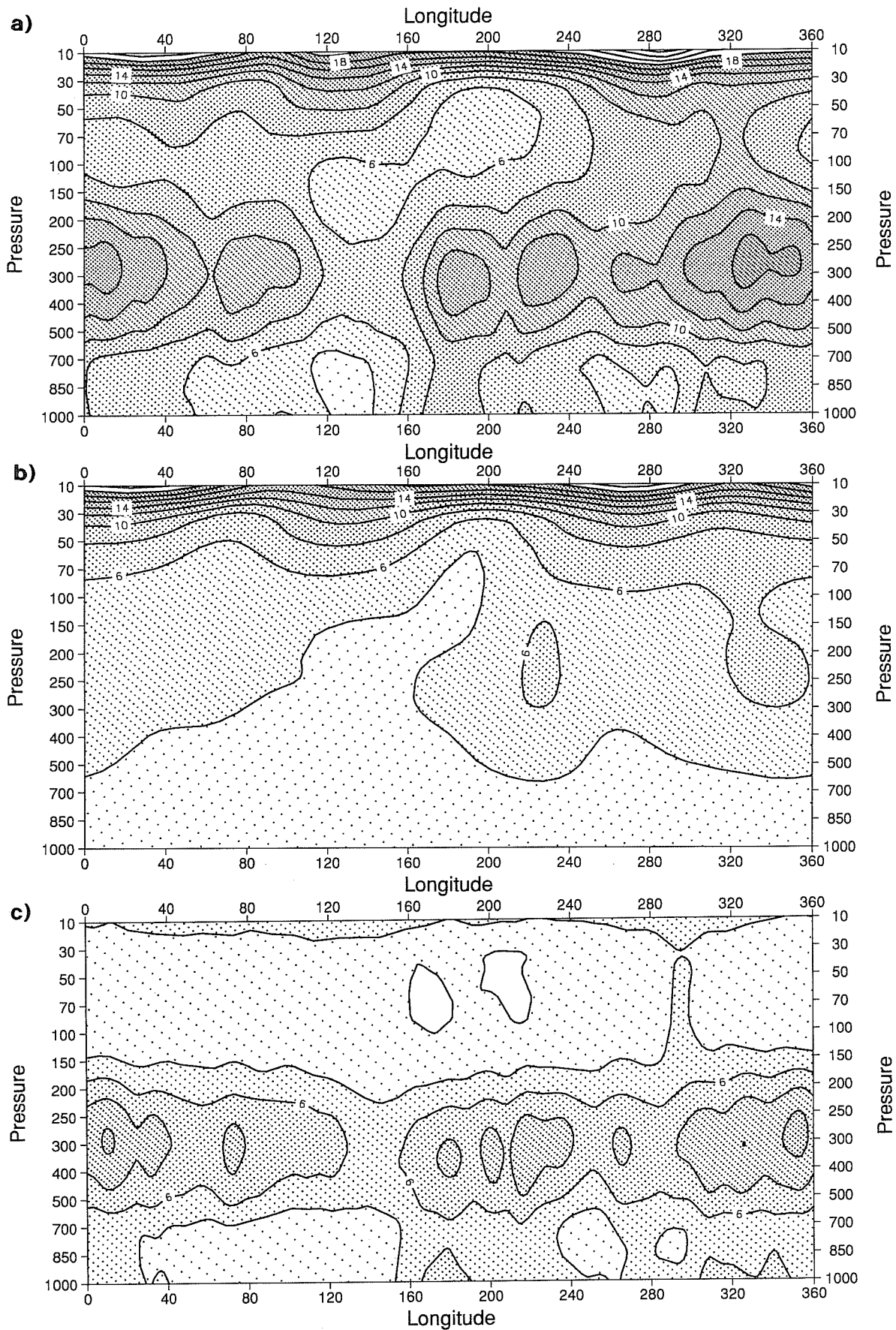


Fig. 10 Longitude-pressure cross section of random forecast errors in terms of standard deviation of forecasts from analyses for winter 1992/93. (a) all waves, (b) long waves (total wavenumber smaller than 7), (c) short waves (total wavenumber larger than 10). Units: dam.

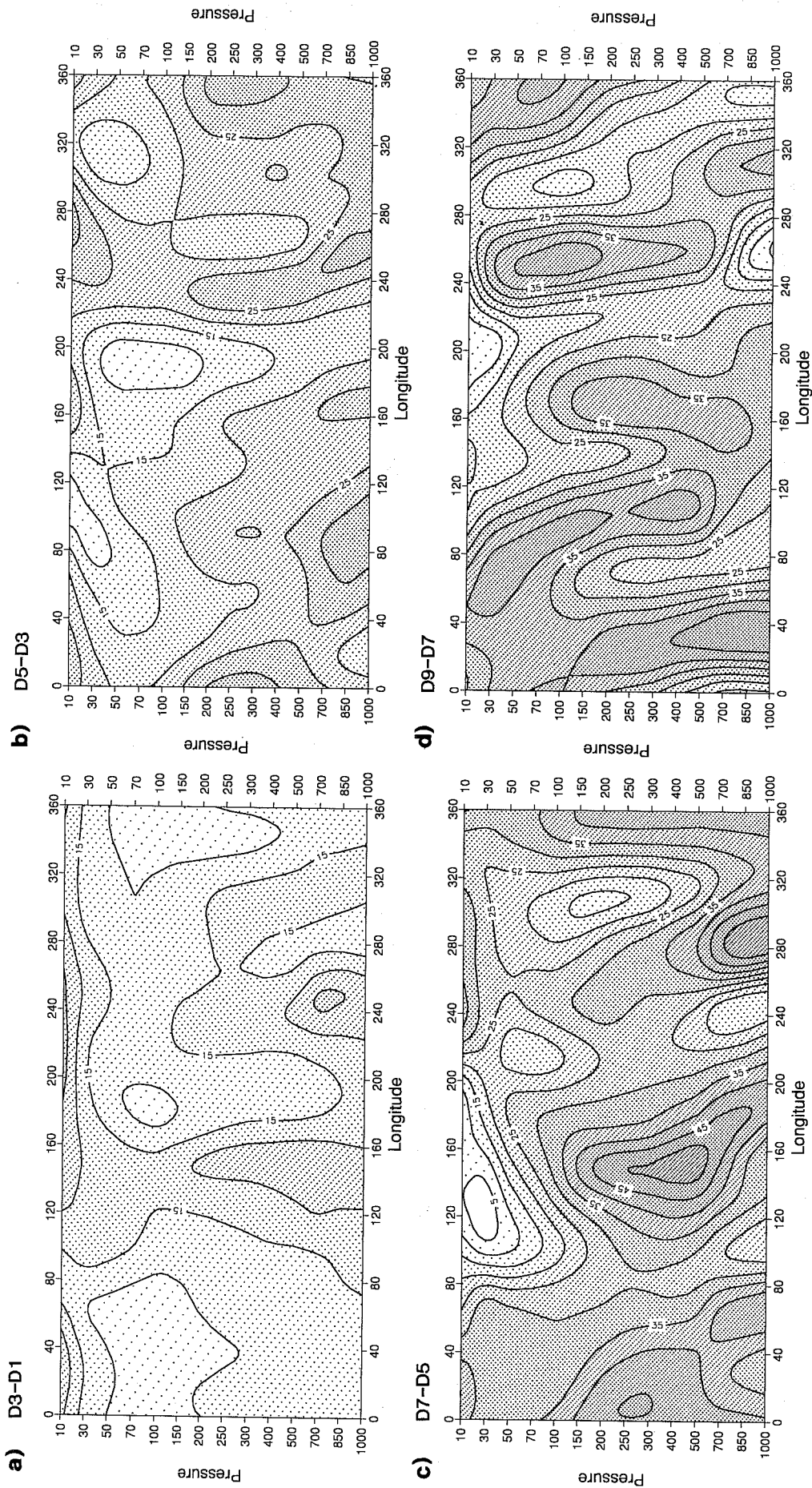


Fig. 11 Longitude-pressure cross section of random height error tendencies for long waves normalized by the atmospheric variability. (a) day-1 to day-3 tendency, (b) day-3 to day-5 tendency, (c) day-5 to day-7 tendency, (d) day-7 to day-9 tendency. Units: darn.

propagation with maximum random error increase being extended upward in the Pacific and in the East Atlantic and European area. Between day-7 and day-9 the maximum error increase has reached the lower stratosphere. The westward tilt of the random error changes suggests that the random errors of the long waves propagate upward more or less parallel the phase lines of the stationary waves. The direction of the long wave random error propagation found here is opposite to the error propagation of systematic errors of the quasi-stationary waves over the European Area.

4. STRATOSPHERIC WARMINGS AND WAVE-MEAN-FLOW INTERACTION

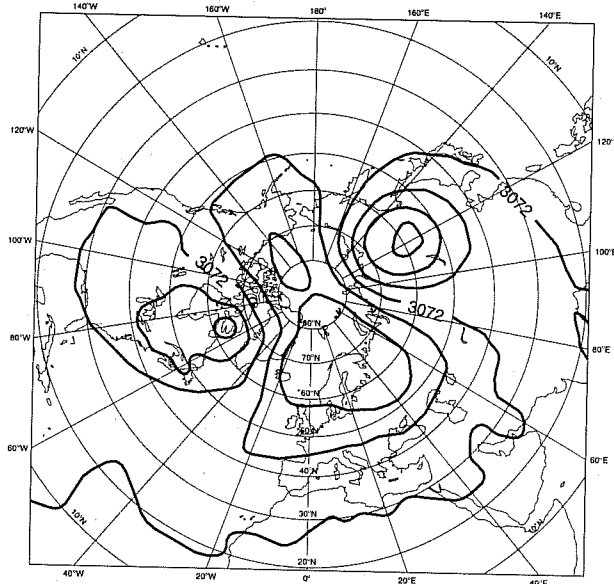
So far the average performance of the ECMWF model for a period of a season has been discussed. During winter in the Northern Hemisphere large circulation changes take place that are known as stratospheric warmings. The deceleration of the stratospheric westerlies is associated with tropospheric planetary waves that propagate into the stratosphere. In the presence of rapid time changes of wave amplitudes or in the presence of damping interactions between the waves and the mean flow are predicted by theory (Andrews and McIntyre, 1976). From these wave-mean-flow interaction between tropospheric planetary waves and the stratospheric mean flow one would expect some dependence of the model performance in the stratosphere on the model performance in the troposphere, particularly with respect to the zonal mean flow.

A major stratospheric warming with a reversal of the westerly flow at 10 hPa occurred in February 1989. The polar vortex which was almost in a climatologically normal position at 13 February split in two parts within a few days and by 23 February (Fig. 12a). The weaker vortex is found over Canada and the more intense one over North Siberia. The zonal flow at high latitudes is completely reversed as the cyclonic circulation is replaced by an anticyclonic one.

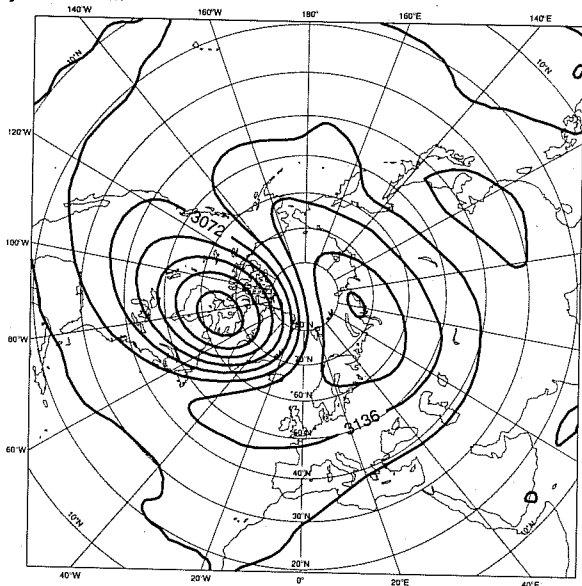
For this case the ten-day operational forecast gave already a good indication of the major circulation change which took place between 13 and 23 February though the details of the predicted circulation pattern were not quite right (Fig. 12b). The vortex close to Canada was too intensive whereas the vortex over Siberia was not deep enough. The five-day forecast from 18 February improved those features, however the tendency to overestimate the intensity of the Canadian vortex and underestimate the Siberian one remained (Fig. 12c).

The change of the mean zonal flow during a stratospheric warming in the Northern Hemisphere can be quite dramatic. Fig. 13a shows a time-pressure section of the zonal mean wind averaged over a latitude band from 65 to 85 degrees north for February 1989. The breakdown of the polar night jet

**a) ECMWF Analysis VT: Thursday 23 February 1989 12z
10 hPa HEIGHT AND TEMP 10**



**b) Monday 13 February 1989 12z ECMWF Forecast t+240 VT: Thursday 23 February 1989 12z
10 hPa HEIGHT**



**c) Saturday 18 February 1989 12z ECMWF Forecast t+120 VT: Thursday 23 February 1989 12z
10 hPa HEIGHT**

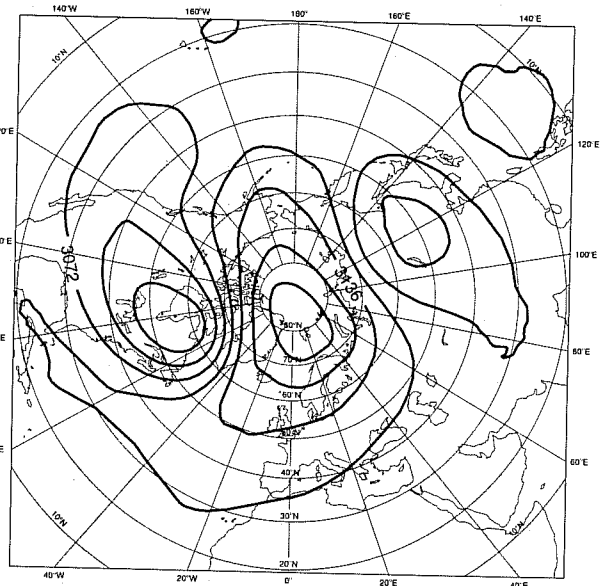
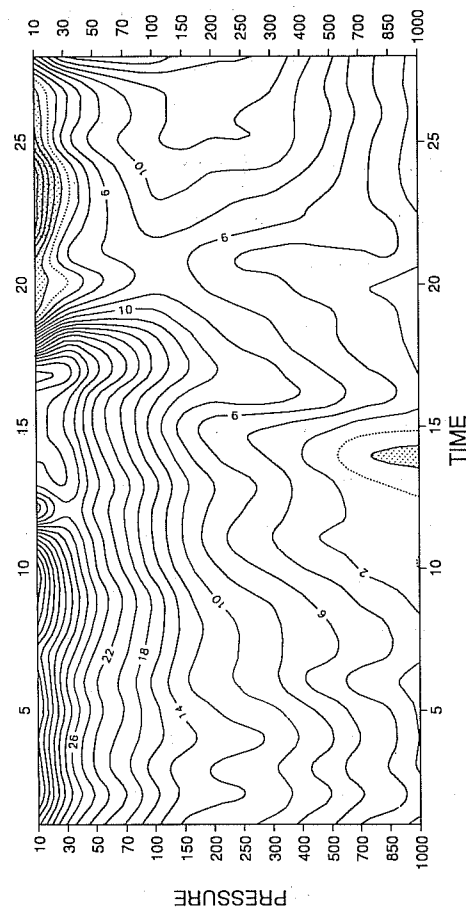
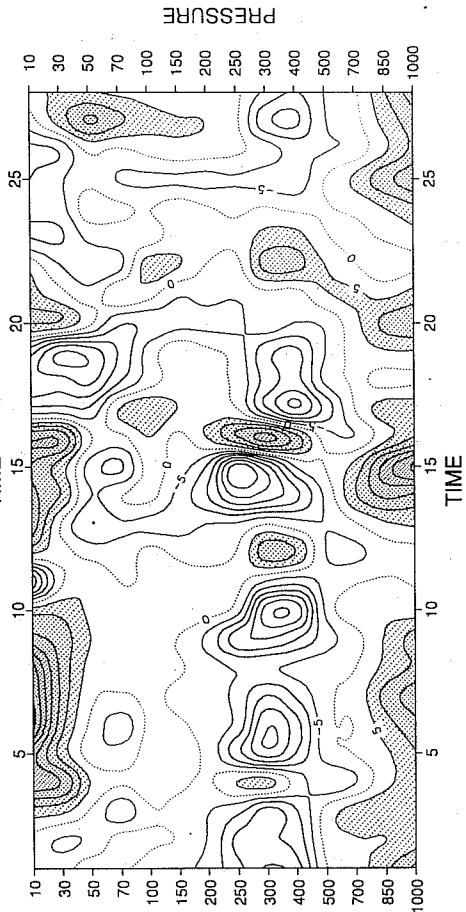


Fig. 12 10 hPa height field. (a) Analysis for 23 February 1989, (b) day 10-forecast from 13 February 1989, (c) day-5 forecast from 18 February 1989. Units: dam.

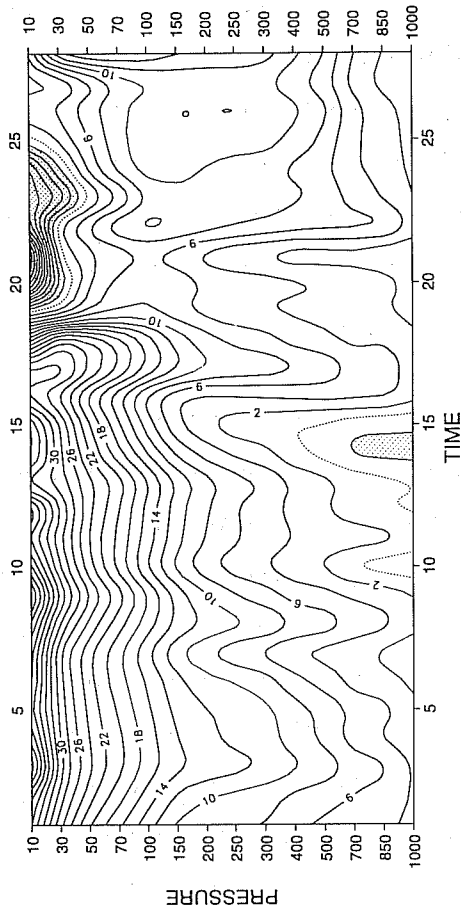
a) D+0 [U] 8902 65-85N



b) Divergence EP 65-85N 8902 D+0



c) D+3 [U] 8902 65-85N



d) Divergence EP 65-85N 8902 D+3

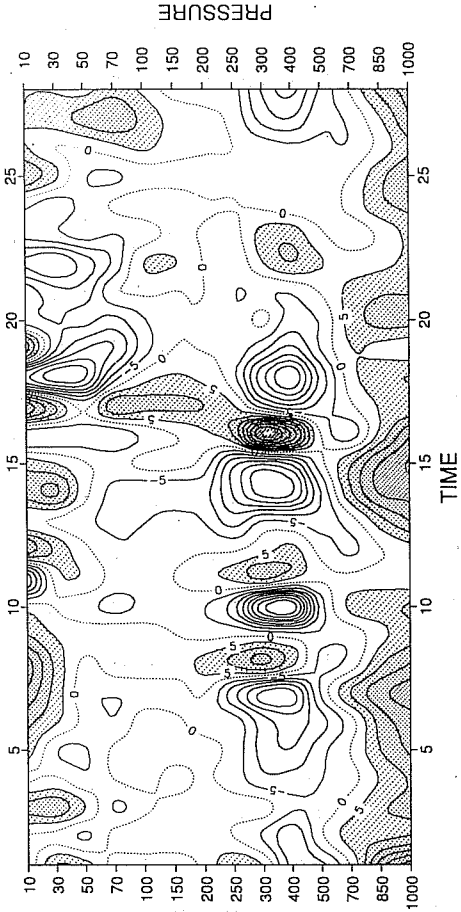


Fig. 13 Time-pressure cross section of the mean zonal wind averaged over 65 to 85 degrees north for February 1989. (a) Analysis, (b) day-5 forecast. Units: m/s.

Fig. 14 Time-pressure cross section of the divergence of the Eliassen-Palm-flux averaged over 65-85 degrees north for February 1989. Units: m/s/day. (a) Analysis, (b) day-3.

starts around 17 February. The westerly zonal flow is reduced in a deep layer extending from the troposphere into the stratosphere, however, a reversal of the zonal flow to easterlies is restricted to stratospheric levels above 30 hPa.

The understanding of the interaction between the planetary waves and the mean flow has been much enhanced by the describing the time changes of the mean zonal flow in the transformed Eulerian formulation (Andrews and McIntyre, 1976; Edmon et al., 1980). The main advantage of this approach is that the forcing of the mean zonal flow by the waves can be expressed by one term, the divergence of the Eliassen-Palm flux (EP-flux). The vector field of the EP-flux, which is defined in the meridional plane, has horizontal and vertical components proportional to the horizontal eddy momentum flux and the vertical eddy heat flux, respectively. In quasi-geostrophic scaling the divergence of the EP-flux is equal to the pole-ward potential vorticity flux. Zonal mean flow changes require non-zero equatorward potential vorticity flux, which may arise from dissipation of waves or transient changes of amplitudes.

The divergence of the EP-flux based on analyzed temperature and wind fields resembles quite closely the observed time variation of the mean zonal flow (Fig. 14a). This is not only the case for the stratosphere but also for the troposphere. Early in the month the divergence of the EP-flux above 50 hPa corresponds to an increase of the zonal flow followed by a short period of flow deceleration around 11 February when the EP-flux was convergent. After an intermediate increase of the westerly flow the major circulation reversal corresponds to maximum convergence of the EP-flux over a deep layer in the stratosphere around 18 February. The vertical structure of the EP-flux divergence and the time change of the mean zonal flow suggest that the deceleration of the westerlies starts in the middle stratosphere before it propagates downwards into the lower stratosphere.

During February 1989 the forecast performance with respect to the stratospheric warming was very good as can be seen from the time-pressure cross section of the zonal mean flow of day-5 forecasts (Fig. 13b). Particularly the major circulation reversal between 17 and 20 February was forecast with nearly perfect timing. A few days later the model tended to overestimate the easterly flow and to extend the flow reversal too deep into the lower stratosphere. For a quantitative comparison of the zonal mean flow errors at day-5 and errors in the divergence of the EP-flux one would have to integrate the EP-flux calculations over the forecast period of 5 days. However, comparing the deviation of the EP-flux divergence at day-3 from the analysis values (Fig. 14b) is already sufficient to relate some forecast errors of the zonal flow at day-5 to errors in the wave-mean-flow interaction. Especially after 20 February the convergence of the EP-fluxes in the forecast became too large, which

contributed to the overestimation of the circulation reversal and to the extension of the easterlies too deep into the lower stratosphere.

Splitting the divergence of the EP-flux into horizontal and vertical components reveals the contributions of different wave properties to errors of the wave-mean-flow interaction (Fig. 15). Errors in the horizontal component of the EP-divergence show a quasi-barotropic structure in the troposphere and a narrow band of large errors close to the top of the model atmosphere. A somewhat different picture arises from errors of the vertical component of the EP-flux divergence, which is proportional to the vertical change of the eddy heat flux. Maximum deviations of forecast values from analysis values are seen in the upper troposphere where the largest random errors of the baroclinic waves were found (see Fig. 10c). A secondary error maximum is again found close to 10 hPa. The overestimation of the easterlies after 20 February seems to be due to a combination of errors in the horizontal and vertical component of the EP-flux divergence.

The transformed Eulerian formulation of the zonal mean momentum equation provides also a very useful framework to discuss seasonal wave-mean-flow interactions. For quasi-geostrophic scaling the EP-flux vectors are parallel to the group velocity of the planetary waves. Therefore the EP-flux vectors shown in Fig.16 for the Northern Hemisphere winter 1992/93 give a good indication of planetary waves propagation into the stratosphere. While these waves penetrate into the stratosphere at middle latitudes they are increasingly refracted towards low latitudes. Convergence of the EP-flux in the lower stratosphere shows that the vertically propagating waves have a decelerating effect on the mean zonal flow. Further up, close to the top of the present operational model where the EP-flux is divergent, the planetary waves tend to accelerate the mean flow.

For the diagnosis of wave-mean-flow interaction errors seasonal calculations for the EP-fluxes have been performed for an ensemble of all day-5 forecasts of winter 1992/93. Fig. 17 shows the difference between the EP-fluxes calculated from day-5 forecasts and from analyses for the winter 1992/93. The differences suggest that the vertically propagating planetary waves are stronger in the middle troposphere, but that they are much weakened close to the tropopause. The resulting reduction of EP-fluxes in the stratosphere has also consequences for the wave-mean-flow interaction, a decreased EP-flux convergence in the lower stratosphere and a decreased EP-flux divergence around 10 and 30 hPa.

Due the density factor EP-fluxes have a general tendency to decrease with height as can be seen from the EP-fluxes from analyses (Fig. 16). The fact that errors of EP-fluxes have a secondary maximum close to the top of the model indicates that errors in that region are not only the consequence of reduced wave propagation from the troposphere. The reflection of vertically propagating waves seem

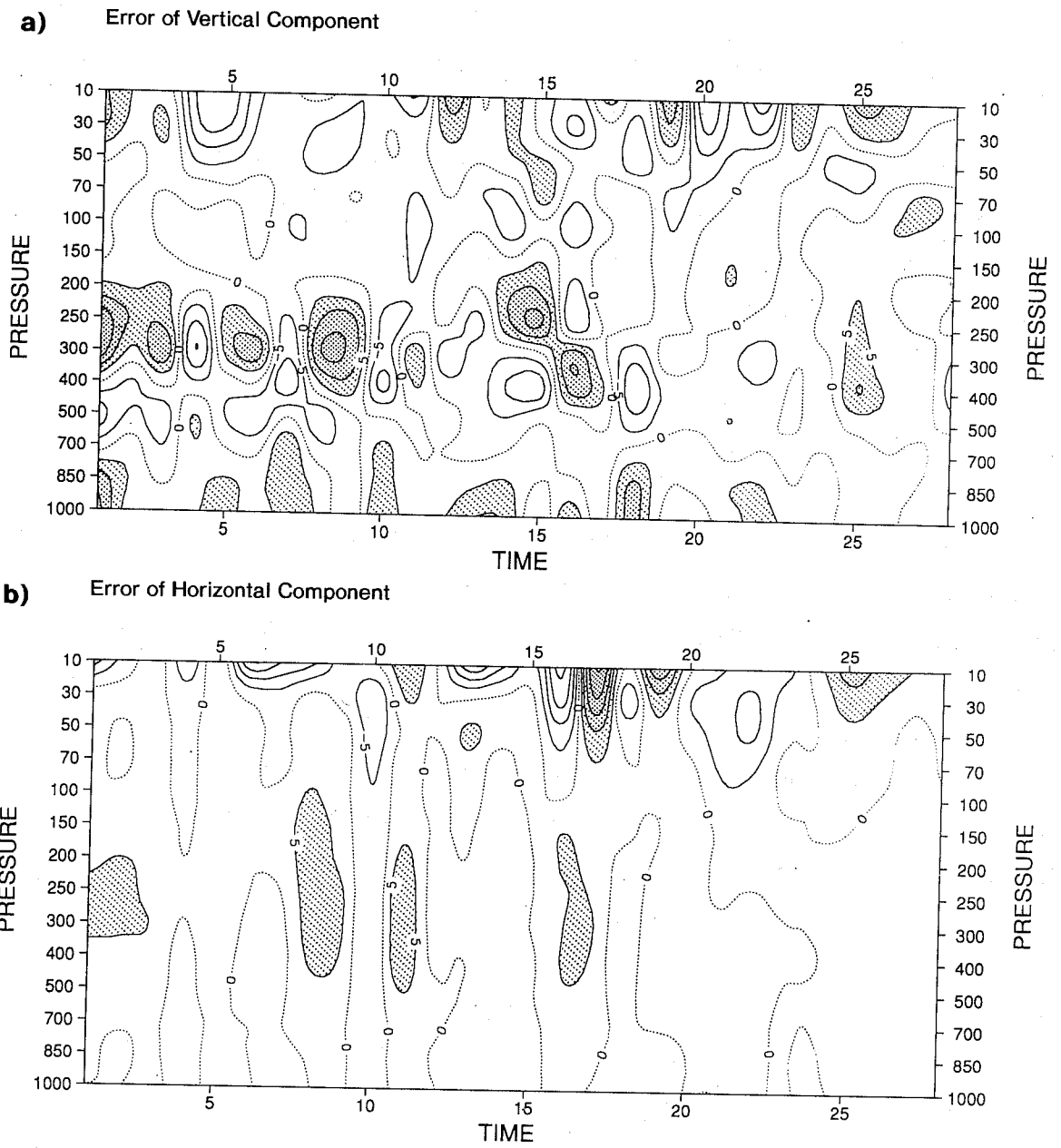


Fig. 15 Time-pressure cross section of the Eliassen-Palm-flux divergence error (D_3-D_0) averaged over 65-85 degrees north for February 1989. (a) Horizontal contribution, (b) vertical contribution. Units: m/s/day.

D+0 Eliassen-Palm DJF 1992/93

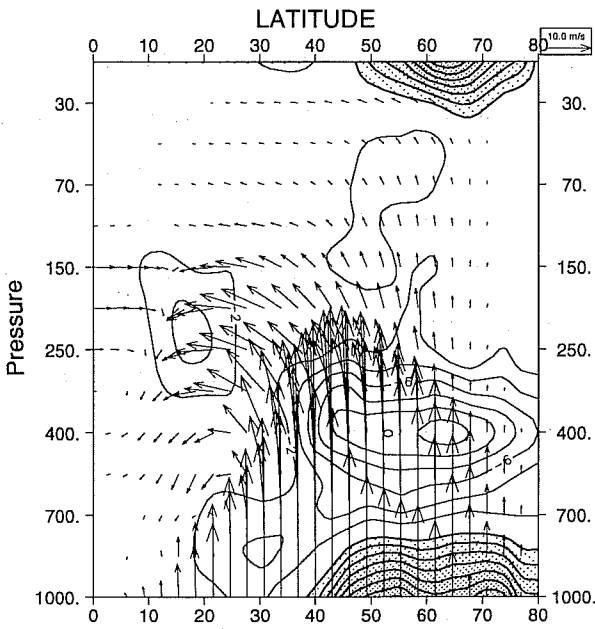


Fig. 16 Eliassen-Palm flux and divergence of the Eliassen-palm-flux for the winter 1992/93. Units of the divergence: m/s/day.

D+5-D+0 Eliassen-Palm DJF 1992/93

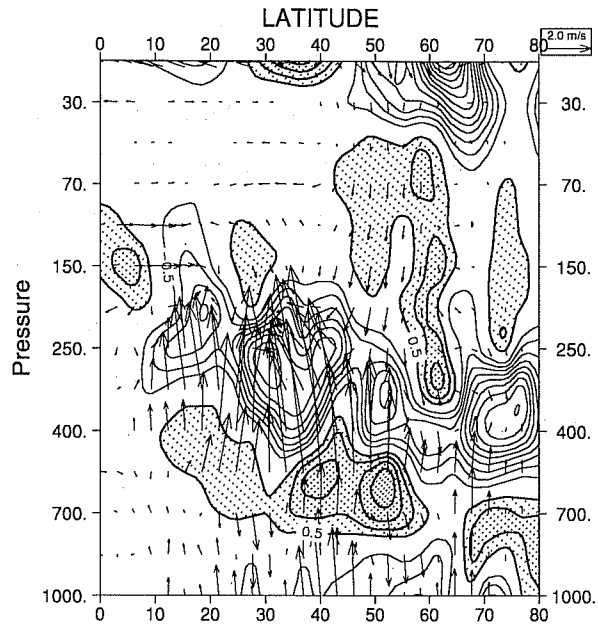
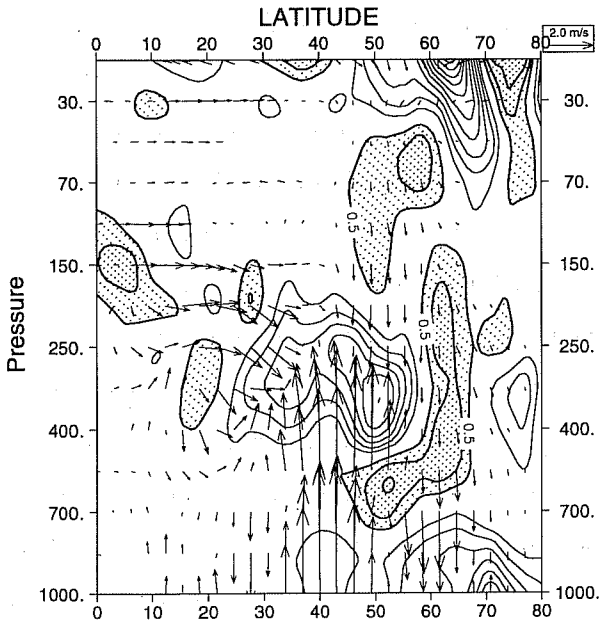


Fig. 17 Day-5 forecast errors of the Eliassen-Palm flux and divergence of the Eliassen-palm-flux for the winter 1992/93. Units of the divergence (m/s/day).

a) D+5-D+0 Eliassen-Palm (Stationary Part) DJF 1992/93



b) D+5-D+0 Eliassen-Palm (Transient Part) DJF 1992/93

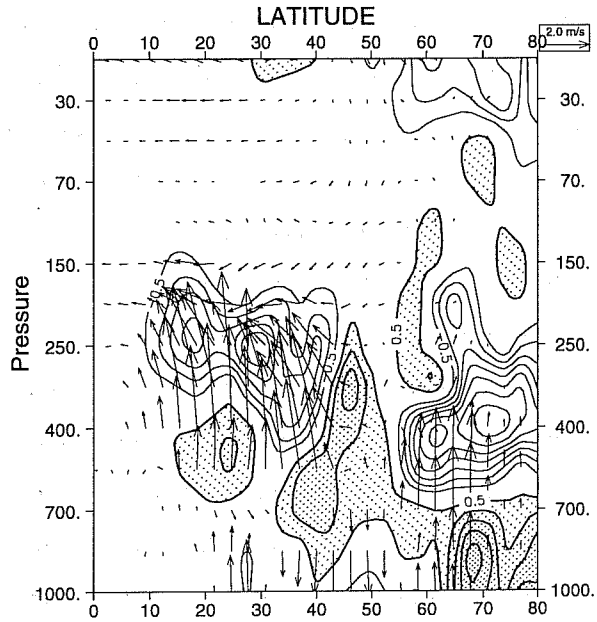


Fig. 18 As Fig. 17, except that errors are split into components arising from (a) stationary waves and (b) transient waves.

to have reduced the EP-fluxes close to the top of the model even further.

The separation of EP-fluxes in transient and stationary part shows that largest day-5 forecast errors in the stratosphere arise from the stationary waves. They contribute to a general weakening of the EP-fluxes in the stratosphere and they also seem to be mainly responsible for large errors close to the top of the model. As one might expect, a spectral decomposition reveals that most of the stratospheric EP-flux errors arise from long waves. The interpretation of the result, that mainly the stationary waves are reflected at the upper boundary causing subsequent problems with the wave-mean-flow interaction, is in agreement with the diagnosis of systematic errors in section 2 from which it was concluded that systematic errors close to the model top propagate downward during the forecast.

5. CONCLUSIONS

The performance of the operational ECMWF model shows a distinct difference between the summer and the winter season. During the summer stratospheric easterlies prevent the propagation of tropospheric waves into the stratosphere. Positive temperature errors in the lower stratosphere and close to the top of the model suggests an imbalance between radiative and dynamical forcing.

During the winter season when the polar night jet is well established the stratospheric circulation is primarily forced by tropospheric waves that are under these conditions able to propagate into the stratosphere. This of course means that tropospheric errors may follow the same track and contaminate the stratospheric forecast. The diagnosis of forecast errors shows that there is a clear signal of upward propagation of random errors of long waves. Maximum increase of errors in the stratosphere was found in the latter period of the operational ten day forecast. The diagnosis of wave-mean-flow interaction using the transformed Eulerian tendency equation for the mean zonal wind shows that the vertically propagating waves are weakened when they pass through the tropopause. A further reduction of EP-fluxes at the upper boundary seems to be due to the reflection of stationary waves at the top model level. In this context it is interesting that systematic errors in the European area showed a tendency to propagate downward from near the top of the model into lower tropospheric layers by day-9. If the Atlantic and European areas are preferred regions of vertical error propagation then a further increase in the vertical resolution in the stratosphere may improve the tropospheric performance particularly in the European area where in the last years the general improvement of medium range forecasts has been well below other regions in the Northern Hemisphere.

REFERENCES

- Andrews, D.G. and M.E. McIntyre, 1976: Planetary waves in horizontal and vertical shear: The generalized Eliassen-palm relation and the mean zonal acceleration. *J. Atmos. Sci.*, 33, 2031-2048.
- Boville, B.A. and D.P. Baumhefner, 1990: Simulated forecast error and climate drift from the omission of the upper stratosphere in numerical models. *Mon. Wea. Rev.*, 118, 1517-1530.
- Doplick, T.G., 1971: The energetics of the lower stratosphere including radiative effects. *Quart. J. Roy. Meteor. Soc.*, 97, 209-237.
- Edmon, H.J. , Jr., Hoskins, B.J., and M.E. McIntyre, 1980: Eliassen-palm cross-sections for the troposphere. *J. Atmos. Sci.*, 37, 2600-2616; corrigendum: 38, 1115 (1981).
- Hartmann, D.L., 1976: The dynamical climatology of the stratosphere in the Southern Hemisphere during late winter 1973. *J. Atmos. Sci.*, 33, 1789-1802.